eLIFE elifesciences.org

RESEARCH ARTICLE

β-blockers augment L-type Ca^{2+} channel activity by targeting spatially restricted β_2AR signaling in neurons

Ao Shen[1,2], Dana Chen[2], Manpreet Kaur[2], Peter Bartels[2], Bing Xu[2,3], Qian Shi[2], Joseph M Martinez[2], Kwun-nok Mimi Man[2], Madeline Nieves-Cintron[2], Johannes W Hell[2], Manuel F Navedo[2], Xi-Yong Yu[1], Yang K Xiang[2,3]*

[1]Key Laboratory of Molecular Target and Clinical Pharmacology, State Key Laboratory of Respiratory Disease, School of Pharmaceutical Sciences & the Fifth Affiliated Hospital, Guangzhou Medical University, Guangzhou, China; [2]Department of Pharmacology, University of California Davis, Davis, United States; [3]VA Northern California Health Care System, Mather, United States

Abstract G protein-coupled receptors (GPCRs) transduce pleiotropic intracellular signals in mammalian cells. Here, we report neuronal excitability of β-blockers carvedilol and alprenolol at clinically relevant nanomolar concentrations. Carvedilol and alprenolol activate β_2AR, which promote G protein signaling and cAMP/PKA activities without action of G protein receptor kinases (GRKs). The cAMP/PKA activities are restricted within the immediate vicinity of activated β_2AR, leading to selectively enhance PKA-dependent phosphorylation and stimulation of endogenous L-type calcium channel (LTCC) but not AMPA receptor in rat hippocampal neurons. Moreover, we have engineered a mutant β_2AR that lacks the catecholamine binding pocket. This mutant is preferentially activated by carvedilol but not the orthosteric agonist isoproterenol. Carvedilol activates the mutant β_2AR in mouse hippocampal neurons augmenting LTCC activity through cAMP/PKA signaling. Together, our study identifies a mechanism by which β-blocker-dependent activation of GPCRs promotes spatially restricted cAMP/PKA signaling to selectively target membrane downstream effectors such as LTCC in neurons.

***For correspondence:** ykxiang@ucdavis.edu

Competing interests: The authors declare that no competing interests exist.

Funding: See page 18

Received: 18 June 2019
Accepted: 13 October 2019
Published: 14 October 2019

Reviewing editor: Mark T Nelson, University of Vermont, United States

Introduction

GPCRs often signal not only through canonical G proteins but also through noncanonical G protein-independent signaling, frequently via G protein receptor kinases (GRKs) and β-arrestins (***Lefkowitz, 2000***; ***Xiang and Kobilka, 2003***). One of the universal features of GPCRs is that they undergo ligand-induced phosphorylation at different sites by either GRKs or second messenger dependent protein kinases such as protein kinase A (PKA). The phosphorylated GPCRs thus may present distinct structural features that favor receptor binding to different signaling partners, engaging distinct downstream signaling cascades (***Reiter and Lefkowitz, 2006***; ***Lefkowitz, 2007***; ***Nobles et al., 2011***). Some ligands can differentially activate a GPCR via a phenomenon known as functional selectivity or biased signaling (***Wisler et al., 2014***; ***Zweemer et al., 2014***). For example, stimulation of β_2 adrenergic receptor (β_2AR), a prototypical GPCR involved in memory and learning in the central nervous system (CNS) and regulation of metabolism and cardiovascular function, promotes phosphorylation by both GRKs and PKA (***Najafi et al., 2016***; ***Mammarella et al., 2016***; ***Fu et al., 2017***; ***Matera et al., 2018***). We have recently identified spatially segregated subpopulations of β_2AR undergoing exclusive phosphorylation by GRKs or PKA in a single cell. These findings indicate specific GPCR subpopulation-based signaling branches can co-exist in a single cell (***Shen et al., 2018***). GRK-mediated phosphorylation promotes pro-survival and cell growth signaling via β-arrestin-

dependent mitogen-activated protein kinase (MAPK/ERK) pathways, prompting the search for biased ligands that preferentially activate β-arrestin pathways (**Luttrell et al., 1999**; **Pierce et al., 2000**; **Kim et al., 2005**; **Ren et al., 2005**; **Zidar et al., 2009**; **Choi et al., 2018**). On the other hand, our recent studies show that the cAMP/PKA-dependent phosphorylation of β_2AR controls ion channel activity at the plasma membrane in primary hippocampal neurons (**Shen et al., 2018**).

β-blockers are thought to reduce cAMP signaling because they either reduce basal activity of βARs or block agonist-induced receptor activation. While β-blockers are successful in clinical therapies of a broad range of diseases, their utility is limited by side effects in both the CNS and peripheral tissues (**Bakris, 2009**; **Gorre and Vandekerckhove, 2010**). Indeed, studies have revealed that some β-blockers display partial agonism and can promote receptor-Gs coupling at high concentrations in vitro (**Yao et al., 2009**; **DeVree et al., 2016**; **Gregorio et al., 2017**). Accordingly, some β-blockers display intrinsic properties mimicking sympathetic activation (sympathomimetic β-blockers) (**Maack et al., 2000**; **Brixius et al., 2001**; **Larochelle et al., 2014**). The mechanism remains poorly understood because classic cAMP assay do not show even minimal cAMP signal induced by these β-blockers (**Maack et al., 2000**; **Brixius et al., 2001**).

In this study, we show that the β-blockers carvedilol and alprenolol can promote Gs protein coupling to β_2AR and cAMP/PKA but not GRK activity at nanomolar concentrations. Thus, these β-blockers are emerging as partial agonists even at low concentrations rather than strict antagonists in mammalian cells. This cAMP/PKA signaling is spatially restricted, selectively promoting phosphorylation of β_2AR and $Ca_V1.2$ by PKA which augments LTCC activity in primary hippocampal neurons. Furthermore, we have engineered a mutant β_2AR that can be selectively activated by carvedilol but not by the orthosteric agonist isoproterenol (ISO) to stimulate PKA but not GRK. Together, these studies identify a unique mechanism by which β-blockers activate β_2AR at low concentrations, which promotes Gs/cAMP/PKA signaling branch and selectively targets downstream LTCC channels in neurons. This observation may also explain sympathomimetic effects of β-blockers in the CNS.

Results

Carvedilol and alprenolol selectively promote β_2AR-mediated PKA-phosphorylation of β_2AR

In this study, we applied two sets of well-characterized phospho-specific antibodies, anti-pS261/262 and anti-pS355/356 to examine a series of β-blockers for their effects on the phosphorylation of β_2AR at its PKA and GRKs sites, respectively (**Shen et al., 2018**; **Tran et al., 2004**; **Tran et al., 2007**). We found that various β-blockers including alprenolol (ALP), carvedilol (CAR), propranolol (PRO) and CGP12177 (177) were able to stimulate phosphorylation of β_2AR at PKA sites expressed in HEK293 cells, similar to the βAR agonist isoproterenol (ISO) (**Figure 1A** and **Figure 1—figure supplement 1A**). In contrast, other β-blockers, that is ICI118551 (ICI), timolol (TIM) and metoprolol (MET), were not able to do so (**Figure 1A**). The ligand-induced phosphorylation of β_2AR was blocked by β_2AR-specific antagonist ICI but not β_1AR-specific antagonist CGP20712A (CGP) (**Figure 1B and C**, and **Figure 1—figure supplement 1B and C**). We chose CAR and ALP for further study. We found that CAR and ALP promoted phosphorylation of β_2AR by PKA even at nanomolar concentrations (**Figure 2A and B**, and **Figure 2—figure supplement 1A and B**), which was paralleled by concentration-dependent increases in phosphorylation of ERK (**Figure 2—figure supplement 2**). The roles of β_2AR and PKA in this phenomenon were confirmed by inhibition of β_2AR with ICI and inhibition of PKA with H89, respectively (**Figure 2C and D**, and **Figure 2—figure supplement 1C and D**). In contrast, those β-blockers induced at best minimal increases in phosphorylation of β_2AR at GRK sites and only at high concentrations, consistent with a previous report (**Wisler et al., 2007**) (**Figure 1A** and **Figure 2—figure supplement 3**). As positive control, the βAR agonist ISO promoted robust increases in both PKA and GRK phosphorylation of the receptors at different concentrations ranging from nanomolar to micromolar (**Figures 1** and **2**, and **Figure 2—figure supplements 2** and **3**). In the CNS, β_2AR emerges as a prevalent postsynaptic norepinephrine effector at glutamatergic synapses (**Davare et al., 2001**; **Joiner et al., 2010**; **Wang et al., 2010**; **Qian et al., 2012**). Consistent with the data from HEK293 cells, we found β-blockers CAR and ALP activated β_2AR and promoted phosphorylation of the receptor by PKA in hippocampal neurons (**Figure 2E**). Together,

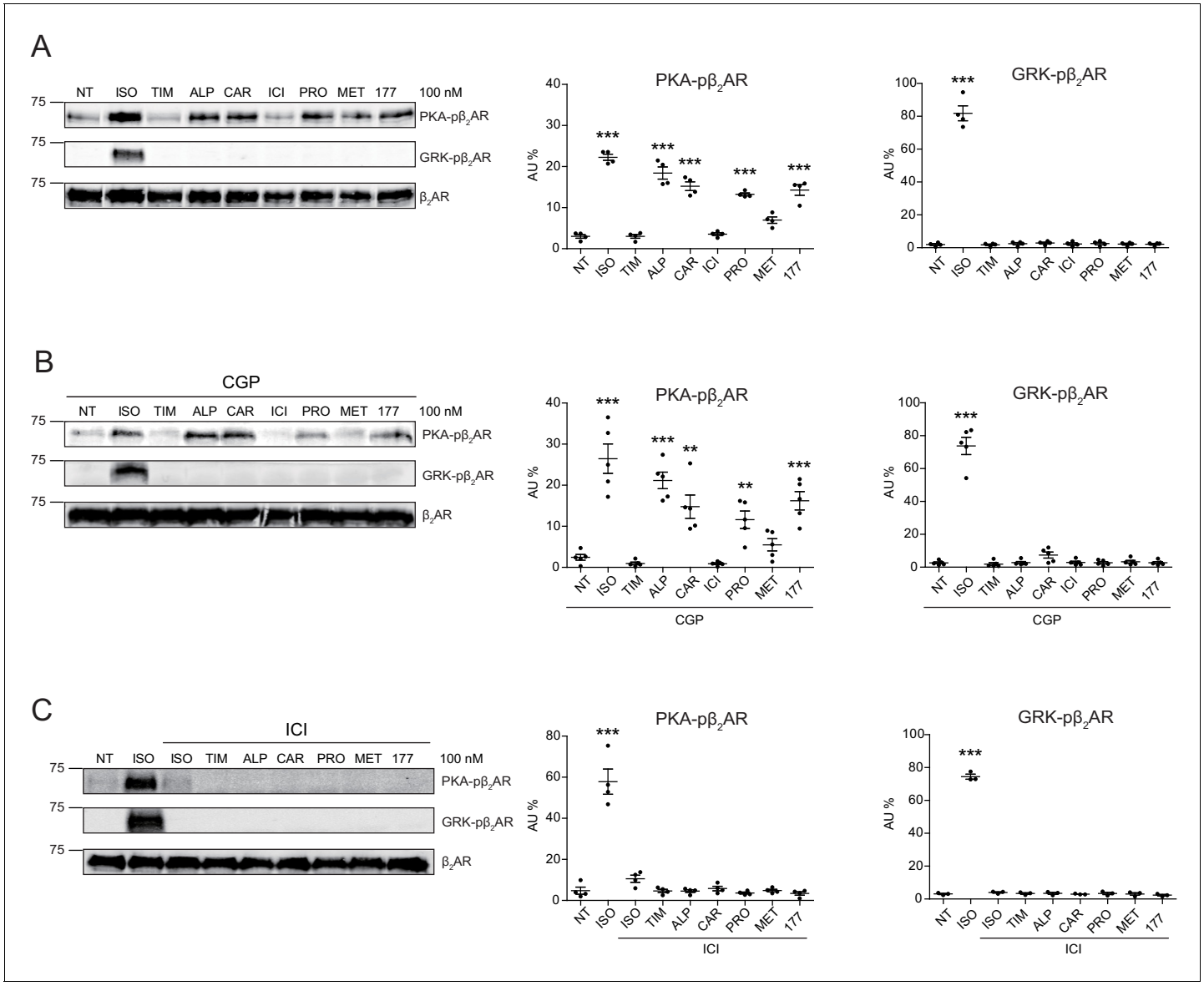

Figure 1. Carvedilol and alprenolol selectively promote phosphorylation of β_2AR at PKA sites. HEK293 cells stably expressing FLAG-tagged β_2AR were either directly stimulated for 5 min with the βAR agonist ISO or different β-blockers at indicated concentrations (**A**) n = 4), or pretreated for 15 min with 1 μM β_1AR antagonist CGP20712A (**B**) n = 5) or 10 μM β_2AR antagonist ICI118551 (**C**) n = 4) before the treatment. The phosphorylation of β_2AR on its PKA and GRK sites were determined with phospho-specific antibodies, and signals were normalized to total β_2AR detected with anti-FLAG antibody. NT, no treatment; ISO, isoproterenol; TIM, timolol; ALP, alprenolol; CAR, carvedilol; ICI, ICI118551; PRO, propranolol; MET, metoprolol; 177, CGP12177; CGP, CGP20712A. Error bars denote s.e.m., *P* values are computed by one-way ANOVA followed by Tukey's test between NT and other groups.

The online version of this article includes the following source data and figure supplement(s) for figure 1:

Source data 1. Excel spreadsheet containing the individual numeric values of phosphorylated β_2AR / total β_2AR relative density analyzed in ***Figure 1***.
Figure supplement 1. Uncropped blots for ***Figure 1***.

these data suggest that certain β-blockers selectively promote PKA phosphorylation of β_2AR in HEK293 and primary hippocampal neurons.

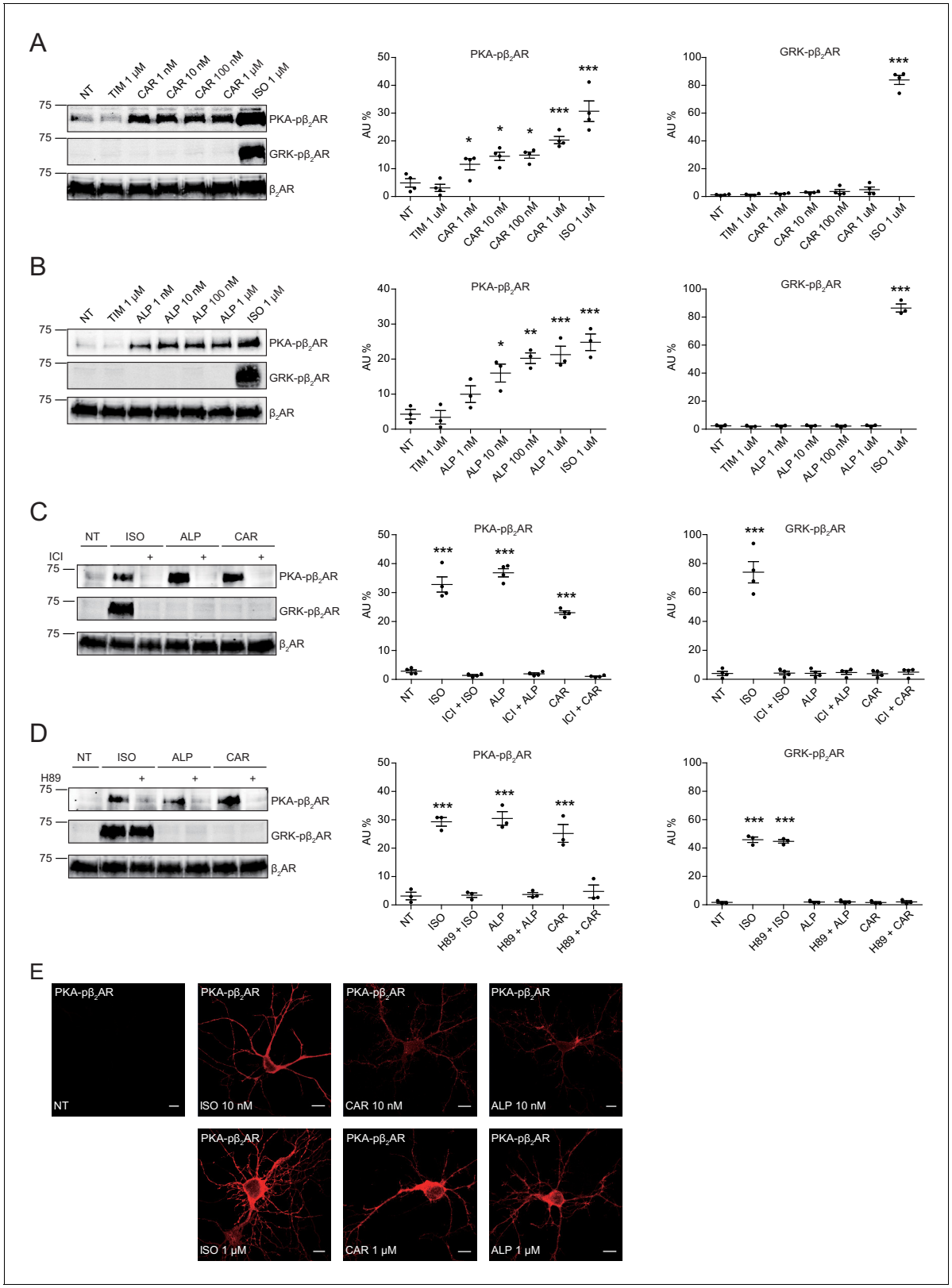

Figure 2. Carvedilol and alprenolol induce concentration-dependent PKA phosphorylation of β_2AR in HEK293 and hippocampal neurons. HEK293 cells stably expressing FLAG-tagged β_2AR were treated with increasing concentrations of CAR (**A**) n = 4) and ALP (**B**) n = 3), or pretreated for 15 min with 10 μM β_2AR antagonist ICI118551 (**C**) n = 4) and PKA inhibitor H89 (**D**) n = 3) before stimulated with 1 μM indicated drugs for 5 min. The phosphorylation of β_2AR on its PKA and GRK sites were determined with phospho-specific antibodies, and signals were normalized to total β_2AR detected with anti-

Figure 2 continued on next page

Figure 2 continued

FLAG antibody. Experiments were performed in the presence of 1 μM β_1AR-selective antagonist CGP20712A to block endogenous β_1AR signaling. NT, no treatment; ISO, isoproterenol; ALP, alprenolol; CAR, carvedilol; ICI, ICI118551. Error bars denote s.e.m., *P* values are computed by one-way ANOVA followed by Tukey's test between NT and other groups. (**E**) Rat hippocampal neurons expressing β_2AR were treated for 5 min with 10 nM or 1 μM indicated drugs on 12 days in vitro (DIV), and immuno-stained for PKA-phosphorylated β_2AR. Confocal images show PKA-phosphorylated β_2AR in agonist- or β-blocker-stimulated neurons have similar distribution. Scale bar, 10 μm. Representative of 6 images for each condition, three experiments.
The online version of this article includes the following source data and figure supplement(s) for figure 2:

Source data 1. Excel spreadsheet containing the individual numeric values of phosphorylated β_2AR / total β_2AR relative density analyzed in ***Figure 2A-D***.
Figure supplement 1. Uncropped blots for ***Figure 2***.
Figure supplement 2. Phosphorylation of ERK and β_2AR at different drug concentrations.
Figure supplement 3. GRK-phosphorylation of β_2AR at different carvedilol treated times.

Carvedilol and alprenolol promote Gsα recruitment to β_2AR and increase spatially restricted cAMP signal

The western blot data on PKA phosphorylation of β_2AR indicates a stimulation of the receptor-mediated Gs/AC/cAMP pathway by these β-blockers. We measured ligand-induced Gsα recruitment to β_2AR with an in situ proximity ligation assay (PLA), which allows direct visualization and quantification of protein-protein interactions. We showed that ISO, CAR and ALP were able to increase the PLA signals between β_2AR and Gsα, indicating recruitment of Gsα to β_2AR (***Figure 3A***). As control, TIM had no effect on the recruitment of Gsα to β_2ARs. The role of Gs/AC in CAR-induced PKA phosphorylation of β_2AR was further validated by AC-specific inhibition with 2',5'-dideoxyadenosine (ddA, ***Figure 3—figure supplement 1***). These data indicate that CAR and ALP are able to stimulate β_2AR-Gs signal to increase PKA phosphorylation of the receptor.

β-blockers have been thought to generally block β_2AR-induced cAMP signal. We hypothesized that the cAMP signal induced by β-blockers is restricted to local plasma membrane domains containing activated receptor, which is not detectable with traditional cAMP assays likely due to limited sensitivity. We applied the highly sensitive FRET-based biosensor ICUE3 to detect the dynamics of cAMP signal in living cells (***DiPilato and Zhang, 2009***; ***De Arcangelis et al., 2009***). The full agonist ISO promoted cAMP signal in HEK293 cells while all β-blockers failed to do so (***Figure 3B***), in agreement with the classic definition of β-blockers. However, when cells were treated with non-selective phosphodiesterase (PDE) inhibitor IBMX, CAR, ALP and CGP12177 were able to induce small but significant cAMP signal in HEK293 cells (***Figure 3C***), indicating a role of PDE in suppressing and restricting the distribution of cAMP in the cells. When β_2AR was exogenously expressed in HEK293 cells, CAR and ALP were able to induce cAMP signal in HEK293 cells even without PDE inhibition (***Figure 3—figure supplement 2***), probably due to insufficient cAMP-hydrolytic activity of endogenous PDEs to counter cAMP production induced from overexpressed β_2AR. We then engineered a targeted cAMP biosensor by fusing the biosensor ICUE3 to the C-terminus of β_2AR (β_2AR-ICUE3), aiming to detect increases of cAMP within the local domain of the receptor. CAR and ALP promoted cAMP signals within the immediate vicinity of activated β_2AR even at nanomolar concentrations (***Figure 3D and E***). The local increases of cAMP were abolished by inhibition of β_2AR with ICI or inhibition of ACs with ddA (***Figure 3E***). We also used two generic plasma membrane (PM) targeted ICUE3 sensors to further characterize how the CAR and ALP generated cAMP signals are localized when compared to the full agonist ISO. Interestingly, neither CAAX-ICUE3 targeting to the non-rafts regions of PM nor LYN-ICUE3 targeting to the rafts regions of PM could sense cAMP induced by CAR and ALP, while ISO induced cAMP were readily detectable on PM (***Figure 3—figure supplement 3***), this further demonstrates that CAR and ALP only promote cAMP within the immediate vicinity of β_2AR. These data confirm that CAR and ALP promote cAMP/PKA activity within the immediate vicinity of activated β_2AR, in contrast to the broad distribution of cAMP/PKA activities induced by ISO in the cells.

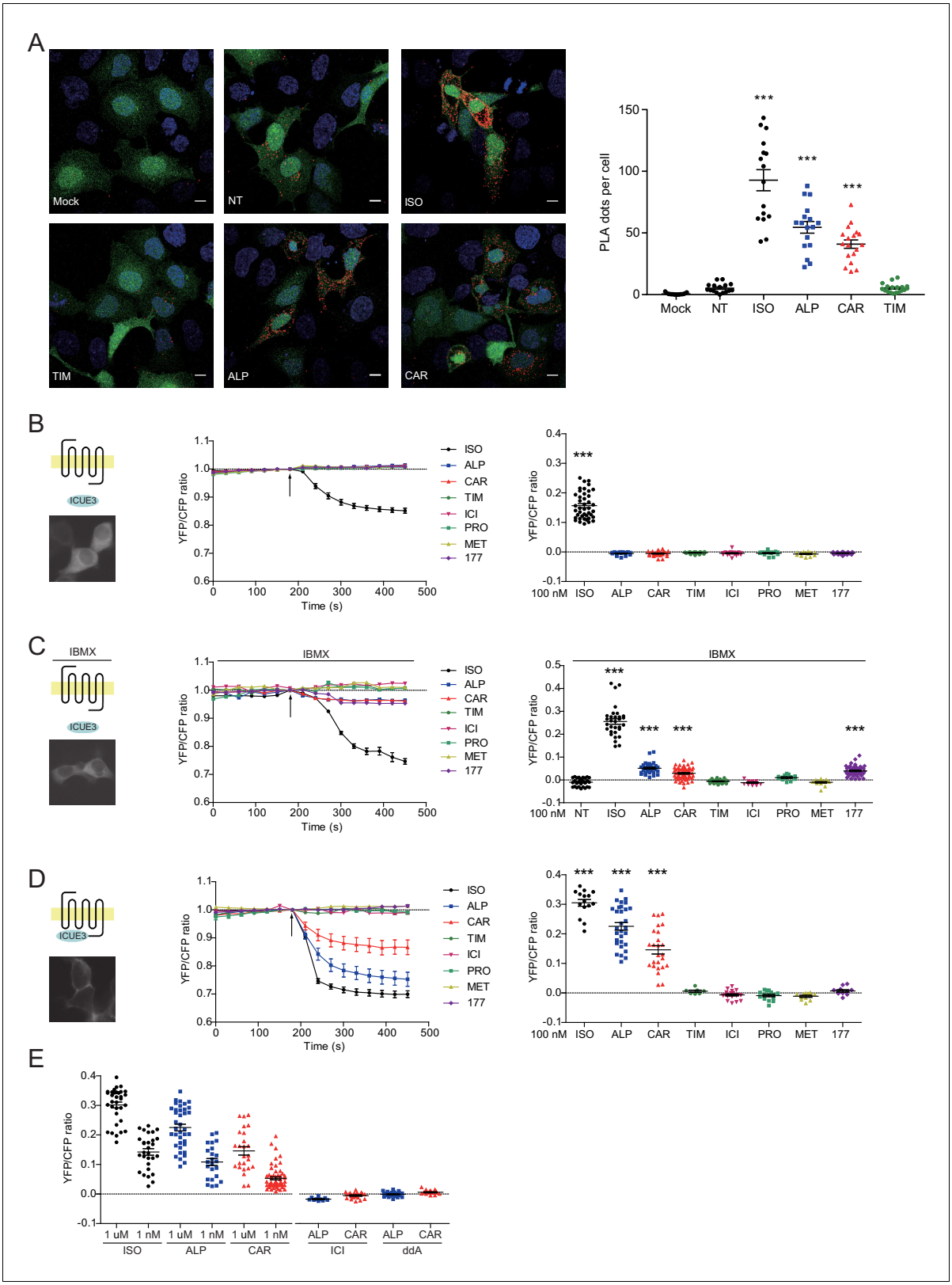

Figure 3. Carvedilol and alprenolol promote Gsα recruitment to β_2AR and increase spatially restricted cAMP signal. (**A**) HEK293 cells co-expressing FLAG-tagged β_2AR, HA-tagged Gsα and EGFP were stimulated with 100 nM ISO or indicated β-blockers for 5 min. In proximity ligation assay (PLA), cells were immuno-stained with HA and β_2AR antibody, nuclei were counterstained with DAPI. The green EGFP signal represents transfected cells, and red PLA signal represents Gsα and β_2AR interactions. Carvedilol and alprenolol promoted Gsα recruitment to β_2AR, but timolol could not. Scale bar, 10

Figure 3 continued on next page

Figure 3 continued

μm. Representative of n = 15, 16, 16, 17, 18 and 18 images respectively, three experiments. (**B–C**) HEK293 cells expressing ICUE3 biosensor were treated with 1 μM ISO or indicated β-blockers (**B**), or together with 100 μM phosphodiesterase inhibitor IBMX (**C**). (**D–E**) HEK293 cells expressing β_2AR-ICUE3 biosensor were treated with indicated concentration of ISO or β-blockers. In some cases, cells were pretreated for 30 min with the β_2AR antagonist ICI (10 μM) or the adenylate cyclase inhibitor ddA (50 μM) before adding β-blockers. Changes in ICUE3 FRET ratio (an indication of cAMP activity) were measured. Experiments were performed in the presence of 1 μM β_1AR-selective antagonist CGP20712A to block endogenous β_1AR signaling. Mock, no primary antibody; NT, no treatment; ISO, isoproterenol; TIM, timolol; ALP, alprenolol; CAR, carvedilol; ICI, ICI118551; PRO, propranolol; MET, metoprolol; 177, CGP12177, IBMX, 3-isobutyl-1-methylxanthine; ddA, 2',5'-dideoxyadenosine. Each dot in the scatter dot plot in **B–E** represents a value from an individual tested cell. Error bars denote s.e.m., *P* values are computed by one-way ANOVA followed by Tukey's test between NT (**A**) or TIM (**B–E**) and other groups.

The online version of this article includes the following source data and figure supplement(s) for figure 3:

Source data 1. Excel spreadsheet containing the individual numeric values of PLA dots / cell number in each raw image analyzed in ***Figure 3A***, and the individual numeric values for maximum FRET responses in ***Figure 3B-E***.

Figure supplement 1. Carvedilol-induced β_2AR phosphorylation is AC-dependent.

Figure supplement 2. Carvedilol- and alprenolol-induced cAMP can be abolished by β_2AR or AC inhibition.

Figure supplement 3. Carvedilol- and alprenolol-induced cAMP are highly restricted.

Carvedilol augments the endogenous β_2AR-dependent PKA phosphorylation of $Ca_V1.2$ and its channel activity in hippocampal neurons

Local cAMP signals possess the potential to selectively regulate downstream effectors in receptor complexes or within the vicinity of activated receptors. In the CNS, β_2AR emerges as a prevalent postsynaptic norepinephrine effector at glutamatergic synapses, where β_2AR functionally interacts with AMPA receptor (AMPAR) and L-type Ca^{2+} channel (LTCC) $Ca_V1.2$, and regulates neuronal excitability and synaptic plasticity (***Davare et al., 2001***; ***Joiner et al., 2010***; ***Wang et al., 2010***; ***Qian et al., 2012***). CAR and ALP, but not TIM significantly increased PKA phosphorylation of S1928 and S1700 of central $\alpha_1$1.2 subunit of $Ca_V1.2$ in hippocampal neurons when both β_2AR and LTCC were endogenously expressed (***Figure 4A***, and ***Figure 4—figure supplement 1A***). However, CAR and ALP failed to promote phosphorylation of the AMPAR subunit GluA1 on its PKA site serine 845 (***Figure 4B***, and ***Figure 4—figure supplement 1B***). Like $Ca_V1.2$, AMPARs are associated with β_2AR, Gs, AC and PKA (***Davare et al., 2001***; ***Joiner et al., 2010***; ***Wang et al., 2010***; ***Qian et al., 2012***). These results indicate high selectivity in targeting downstream substrates by this β-blocker-induced signaling in hippocampal neurons. Meanwhile, the CAR and ALP-induced PKA phosphorylation of LTCC were blocked by β_2AR inhibitor ICI, AC inhibitor ddA, and PKA inhibitor H89, but not CaMKII inhibitor KN93, validating the activation of β_2AR-cAMP-PKA pathway (***Figure 4C***, and ***Figure 4—figure supplement 1C***). We then examined the effects of CAR on PKA-dependent activation of LTCC $Ca_V1.2$ channels using cell-attached single channel recordings in hippocampal neurons. As shown before, ISO stimulates LTCC activity (***Figure 5***) (***Shen et al., 2018***; ***Davare et al., 2001***). Consistent with the phosphorylation data, CAR but not TIM significantly increased the open probability, channel availability and mean ensemble average of endogenous LTCC in rat hippocampal neurons (***Figure 5*** and ***Figure 5—figure supplement 1***). CAR stimulated channel activity when present in the patch pipette solution but not when applied outside the patch via bath perfusion (***Figure 5*** and ***Figure 5—figure supplement 1D***). Moreover, backfilling experiments with CAR found that L-type channels activity was relatively low at the beginning of the recording but then it significantly increased as the drug diffused to the pipette tip (***Figure 5F–G*** and ***Figure 5—figure supplement 1C***). Consistent with our hypothesis and prior studies (***Davare et al., 2001***), ISO applied outside the patch via bath perfusion was still able to stimulate LTCC activity (***Figure 5—figure supplement 1B***). These data indicate that CAR promotes spatially restricted cAMP/PKA activities for selective augmentation of LTCC activities in neurons. We further found that the activation of LTCC by CAR promoted cell death in cortical neuron cultures, and inhibition of β_2AR or LTCC counteracted carvedilol-induced neuronal toxicities (***Figure 5—figure supplement 2***).

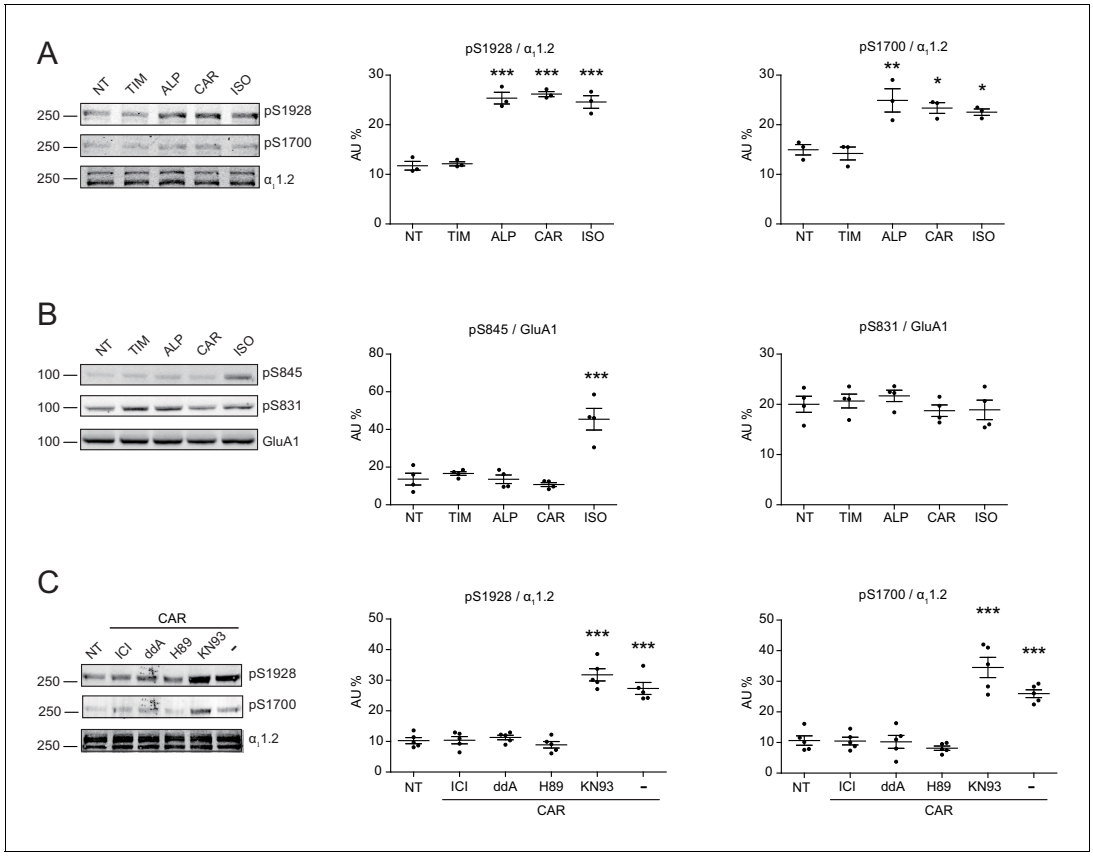

Figure 4. Carvedilol promotes endogenous β_2AR-dependent phosphorylation of LTCC $\alpha_1$1.2 by PKA in neurons. (**A**) Rat neurons on 10–14 days in vitro (DIV) were treated for 5 min with 1 μM indicated drugs. The phosphorylation of endogenous LTCC $\alpha_1$1.2 subunit was determined with phospho-specific antibodies, and normalized to total $\alpha_1$1.2, n = 3. (**B**) Rat neurons on 10–14 DIV were treated for 5 min with 1 μM indicated drugs. The phosphorylation of endogenous AMPAR GluA1 subunit was determined with phospho-specific antibodies, and signals were normalized to total GluA1, n = 4. (**C**) Neurons were pretreated for 30 min with 10 μM β_2AR inhibitor ICI, 50 μM AC inhibitor ddA, 10 μM PKA inhibitor H89 or 10 μM CaMKII inhibitor KN93 and then stimulated with 1 μM CAR for 5 min. Carvedilol-induced LTCC phosphorylation depends on endogenous β_2AR, AC and PKA, but not CaMKII, n = 5. NT, no treatment; ISO, isoproterenol; TIM, timolol; ALP, alprenolol; CAR, carvedilol. Error bars denote s.e.m., *P* values are computed by one-way ANOVA followed by Tukey's test between NT and other groups.

The online version of this article includes the following source data and figure supplement(s) for figure 4:

Source data 1. Excel spreadsheet containing the individual numeric values of phosphorylated $a_1$1.2 or GluA1 / total $a_1$1.2 or GluA1 relative density analyzed in ***Figure 4***.

Figure supplement 1. Uncropped blots for ***Figure 4***.

Carvedilol but not isoproterenol selectively activates a mutant β_2AR to augment LTCC activity in neurons

Structure-functional analyses of β_2AR have previously revealed distinct residues important for binding to catecholamines and β-blockers (***Strader et al., 1989***; ***Liapakis et al., 2000***; ***Warne et al., 2012***; ***Ring et al., 2013***). We hypothesized that mutation of Ser204 and Ser207 sites within β_2AR binding pocket would abolish receptor hydrogen bonds with the catecholamine phenoxy moieties, thus reducing binding affinity to agonist ISO while having no effect on β-blocker binding (***Figure 6A***). Such a mutant β_2AR could thus be selectively activated by CAR. We co-expressed the cAMP biosensor ICUE3 together with either wild-type (WT) β_2AR or mutant S204A/S207A β_2AR in MEF cells lacking endogenous β_1AR and β_2AR (DKO) to detect receptor signaling induced by different ligands. The mutant S204A/S207A β_2AR induced a moderate cAMP signal at high but not low concentrations of ISO (***Figure 6B***). In contrast, after stimulation with CAR, the β_2AR mutant S204A/S207A promoted significant cAMP signals at nanomolar concentrations; the overall concentration response curve was similar to those induced by WT β_2AR (***Figure 6B***). Accordingly, the ISO-induced

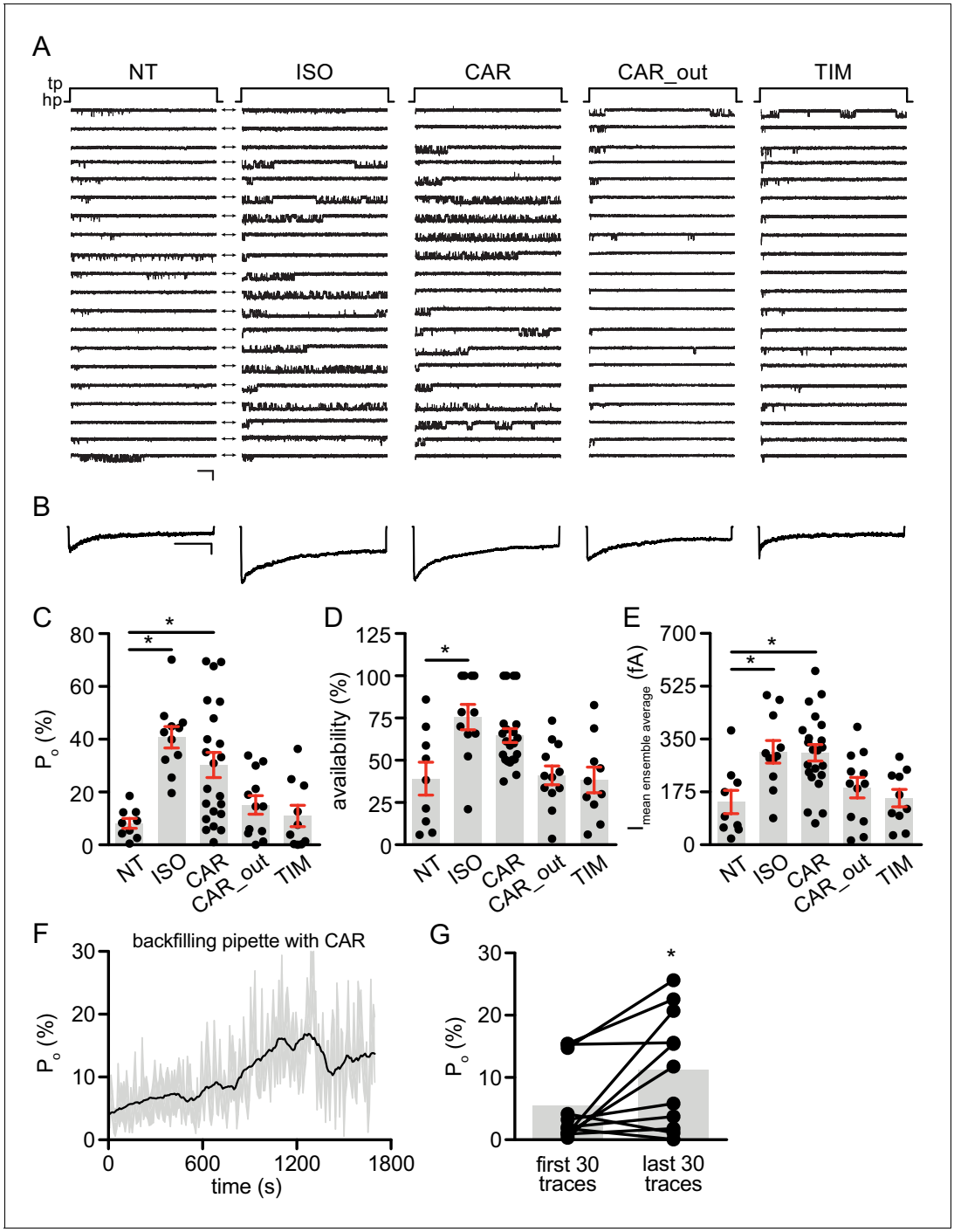

Figure 5. Carvedilol augments LTCC $Ca_V1.2$ channel activity in neurons. (**A**) Representative single channel recordings of LTCC $Ca_V1.2$ currents using 110 mM Ba^{2+} as charge carrier in rat hippocampal neurons on 7–10 days in vitro (DIV) after depolarization from −80 (hp) to 0 mV (tp) in control patches (NT), patches containing 1 µM isoproterenol (ISO), 1 µM carvedilol (CAR) or 1 µM timolol (TIM) in the patch pipette or after addition of 1 µM CAR to the bath while the patch pipette contained a control pipette solution (CAR_out). Shown are 20 consecutive sweeps from representative experiments. Arrows throughout the figure indicate the 0-current level (closed channel). Scale bar denotes 2 pA and 200 ms. (**B**) Ensemble average currents as determined from all sweeps recorded for all the experimental conditions. Scale bar denotes 50 fA and 400 ms. (**C–E**) Mean ± s.e.m. for (**C**) P_o (%), (**D**) availability (i.e. likelihood that a sweep had at least one event) (%) and (**E**) the mean ensemble average current (fA) for each experimental condition. *p<0.05 with Kruskal Wallis – Dunn's multiple comparison test. Sweep and n numbers as well as summary statistics are in ***Supplementary file 1***. (**F**) Ensemble P_o versus time measurements obtained with a pipette backfilled with 1 µM CAR. The solid dark line represents the mean P_o over time and the gray area is the s.e.m. at each time point. The mean line was smoothed to 15 neighbors on each size with a second order polynomial smoothing in

Figure 5 continued on next page

Figure 5 continued

PRISM for representation purposes only. (**G**) Mean Po of the first 30 traces versus the last 30 traces obtained with a pipette backfilled with 1 μM CAR. The gray boxes highlight the mean on each group. n = 11 patches. *p<0.05 with Mann-Whitney test.

The online version of this article includes the following source data and figure supplement(s) for figure 5:

Source data 1. Excel spreadsheet containing the individual numeric values of Po, availability and current analyzed in ***Figure 5***C-G.
Figure supplement 1. Over-time effect of carvedilol on LTCC of neurons recorded in the cell attached configuration without using BayK.
Figure supplement 2. Inhibition of β_2AR or LTCC counteracts carvedilol-induced cell death of cultured cortical neurons.

PKA phosphorylation of β_2AR S204A/S207A mutant was selectively abolished at nanomolar concentrations. At higher concentrations, ISO was able to induce reduced PKA phosphorylation of the β_2AR S204A/S207A mutant when compared to WT β2AR, consistent with the data of cAMP signals (***Figure 6C***, and ***Figure 6—figure supplement 1A***). Meanwhile, ISO failed to induce GRK phosphorylation of β_2AR S204A/S207A mutant at different concentrations (***Figure 6C***). In comparison, CAR induced equivalent PKA phosphorylation of β_2AR WT and S204A/S207A mutant at different concentrations (***Figure 6D***, and ***Figure 6—figure supplement 1B***). These data suggest that CAR, but not ISO selectively activates the S204A/S207A mutant β_2AR at nanomolar concentrations. We then tested the effects of β_2AR S204A/S207A mutant on LTCC channel activity after treatment with CAR in hippocampal neurons. In DKO neurons expressing the mutant S204A/S207A β_2AR, CAR, but not ISO (30 nM) promoted PKA phosphorylation of LTCC $\alpha_1$1.2 (***Figure 7A and B*** and ***Figure 7—figure supplement 1***). In agreement, CAR, but not ISO significantly increased the open probability, channel availability and mean ensemble average of LTCC (***Figure 7C–7G***). Together, CAR but not ISO selectively activates the S204A/S207A mutant β_2AR at low concentrations and increases channel opening probabilities.

Discussion

In a classic view, agonist stimulation promotes both PKA and GRK phosphorylation of activated GPCRs. Although previous studies have reported that some β-blockers promote βAR-Gs coupling and thus might display partial agonism, this phenomenon is only observed at high concentrations and in vitro with reconstituted systems (***Yao et al., 2009***; ***DeVree et al., 2016***; ***Gregorio et al., 2017***). In this study, using a combination of highly sensitive tools such as engineered FRET-based cAMP sensors and single channel recording together with detection by phospho-specific antibodies, we show for the first time that β-blockers such as CAR and ALP can promote receptor-Gs coupling at nanomolar concentrations in living cells, which is clinically relevant in contrast to superphysiological concentrations in previous studies. In detail, as low as 1 nM alprenolol as well as 1 nM carvedilol induce 20–40% of maximal effects (as obtained with 1 μM isoproterenol) with respect to phosphorylation of β_2AR by PKA and to cAMP production detected by the ICUE3 sensor coupled to β_2AR. Unlike agonists, activation of β_2AR by β-blockers selectively transduce G protein/cAMP/PKA signaling but not GRK signaling. More importantly, the β_2AR-induced cAMP signal is highly spatially restricted to the local domain of activated β_2AR, which selectively promotes activation of receptor-associated LTCC but not receptor-associated AMPAR, two downstream ion channels essential for adrenergic regulation of neuronal excitability in hippocampal neurons. The differential signaling by carvedilol with respect to LTCC and AMPAR is especially remarkable because both channels form complexes with β_2AR that are localized within dendritic spines. Moreover, we have engineered a mutant β_2AR that is selectively activated by β-blockers but not by catecholamines at low concentration. Our study defines CAR and ALP as Gs-biased partial agonists of βAR for highly spatially restricted cAMP/PKA signaling to Ca_V1.2 in neurons. The study exemplifies a unique mechanism by which β-blockers shape the compartmentalization of βAR signaling and a highly restrictive distribution of ligand-induced activation of GPCR targeting a specific downstream effector.

PKA-mediated phosphorylation is thought to play critical roles in heterologous desensitization of GPCRs and in receptor switching from Gs to Gi coupling (***Daaka et al., 1997***; ***Zamah et al., 2002***), whereas GRK-mediated phosphorylation is implicated in β-arrestin recruitment and β-arrestin-dependent ERK activation (***Luttrell et al., 1999***; ***Pierce et al., 2000***; ***Kim et al., 2005***; ***Ren et al., 2005***; ***Zidar et al., 2009***; ***Choi et al., 2018***). We have recently characterized that PKA and GRKs phosphorylate distinct subpopulations of β_2AR in a single fibroblast or neuron (***Shen et al., 2018***). While GRK

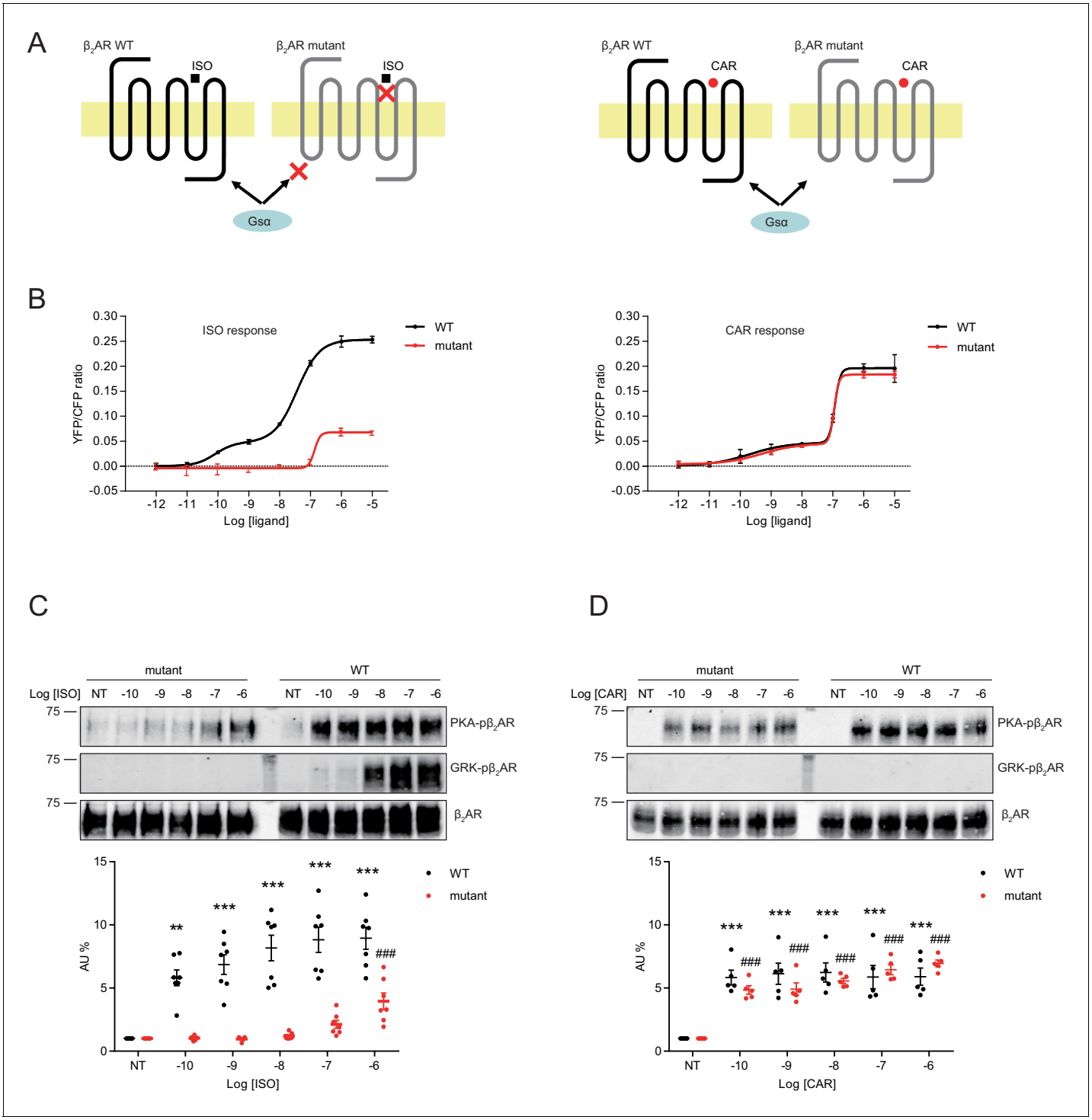

Figure 6. A mutant β_2AR is selectively activated by carvedilol but not isoproterenol. (**A**) Schematic of an engineered β_2AR with S204/207A double serine mutations that loses high affinity binding to ISO but not CAR at nanomolar range. (**B**) cAMP biosensor ICUE3 and β_2AR wild-type (WT) or mutant were co-expressed in MEF cells lacking both β_1AR and β_2AR. Changes of cAMP FRET ratio by increasing concentrations of ISO or CAR were measured. n = 5–29 cells. (**C–D**) HEK293 cells stably expressing FLAG-tagged β_2AR WT or mutant were stimulated for 5 min with increasing concentrations of ISO (**C**), n = 7) or CAR (**D**), n = 5). The phosphorylation of β_2AR on its PKA and GRK sites were determined with phospho-specific antibodies, and signals were normalized to total β_2AR detected with anti-FLAG antibody. Experiments were performed in the presence of 1 μM β_1AR-selective antagonist CGP20712A to block endogenous β_1AR signaling. NT, no treatment; ISO, isoproterenol; CAR, carvedilol. Error bars denote s.e.m., *P* values are computed by one-way ANOVA followed by Tukey's test between NT and other concentrations.

The online version of this article includes the following source data and figure supplement(s) for figure 6:

Figure 6 continued on next page

Figure 6 continued

Source data 1. Excel spreadsheet containing the individual numeric values for maximum FRET responses in ***Figure 6B***, and the individual numeric values of phosphorylated β_2AR / total β_2AR relative density analyzed in ***Figure 6C-D***.
Figure supplement 1. Uncropped blots for ***Figure 6C and D***.

phosphorylation of β_2AR is only observed at high concentrations of agonists, PKA phosphorylation can be induced with minimal doses of agonist (***Shen et al., 2018***; ***Tran et al., 2004***; ***Tran et al., 2007***; ***Liu et al., 2009***). Here, our data show CAR does not promote GRK phosphorylation at low concentrations and induces a slow and minimal GRK effect at high concentrations when compared to those induced by ISO. The CAR-induced GRK effects are minimally related to the PKA effects. Previously, CAR has been recognized as a biased β-blocker that preferentially activates β-arrestin/ERK pathways (***Wisler et al., 2007***; ***Kim et al., 2008***). Despite the prominent role of GRK phosphorylation in full agonist ISO-induced β_2AR-β-arrestin/ERK signaling, our data clearly indicate that GRK phosphorylation of β_2AR is not necessary for CAR-induced activation of ERK, consistent with a recent study showing a distinct general mechanism of β-arrestin activation that does not require the GRK-phosphorylated tail of different GPCRs (***Eichel et al., 2018***). Meanwhile, other studies show that in the absence of all G proteins, GPCRs fail to transduce β-arrestin/ERK signaling (***Grundmann et al., 2018***). These data indicate the necessity of G proteins in GPCR-induced arrestin activation. In our study, we observed a concentration-dependent correlation between PKA phosphorylation of β_2AR with ERK activity induced by β-blockers, suggesting the potential role of Gs and PKA in CAR-induced β_2AR-β-arrestin/ERK signaling are overlooked. In comparison, Gi is not required for CAR-induced β_2AR/β-arrestin signaling even though CAR induces Gi recruitment to β_1AR for transducing β_1AR/β-arrestin signaling (***Wang et al., 2017***). Moreover, our results are also in line with a recent report that activation of β_2AR with as low as femtomolar concentrations of ligands causes sustained ERK signaling (***Civciristov et al., 2018***), further support a PKA but GRK-dependent mechanism in GPCR-induced ERK activation. Future studies will help us understand how ligand-induced GPCRs utilize distinct mechanisms in activating β-arrestin/ERK pathway.

Engineered GPCRs have been widely applied in investigating structural and biological processes and behaviors by precisely controlling specific GPCR signaling branches (***Lee et al., 2014***). Previous mutagenesis studies have shown that β_2AR with S204/207A mutation loses binding to adrenaline but still binds with several β-blockers including ALP (***Liapakis et al., 2000***). Based on this and recent advances in βAR structures with agonists and β-blockers (***Warne et al., 2012***; ***Ring et al., 2013***), we have generated a S204/207A mutant that bestow β_2AR with the ability to be selectively activated by β-blockers such as CAR and to transduce cAMP/PKA signaling. At nanomolar concentrations, while ISO fails to stimulate PKA phosphorylation of the S204/207A mutant β_2AR, the mutant receptor still retains CAR-induced stimulation of PKA-phosphorylation of the receptor. The CAR-induced activation of mutant β_2AR triggers the β_2AR/Gs/cAMP/PKA signaling pathway and selectively targets downstream effectors in primary hippocampal neurons. Interestingly, the S204/207A β2AR mutant is not only refractory to its agonists but also completely lost both ISO- and CAR-induced GRK-phosphorylation of β_2AR. Further studies comparing this mutant with previous reported β_2AR-TYY and Y219A mutants that lack Gs and GRKs coupling, respectively (***Choi et al., 2018***; ***Shenoy et al., 2006***), will facilitate the analysis of the physiological relevance of Gs/cAMP/PKA-dependent and GRK-dependent signaling pathways and enable researchers to explore β-arrestin/ERK pathway devoid of individual signaling branches.

β-blockers are a standard clinical treatment in a broad range of diseases. Many β-blockers possess intrinsic sympathomimetic activities (***Bakris, 2009***; ***Gorre and Vandekerckhove, 2010***), which are problematic due to the side effects through stimulation of βARs (***Bakris, 2009***; ***Gorre and Vandekerckhove, 2010***), a feature that limits the clinical utility of the drugs. Here, we show that β-blockers promote activation of β_2AR by recruiting Gs that selectively transduces cAMP/PKA signal but not GRK signal. Meanwhile, binding of β-blockers to β_1AR has been shown to enhance cAMP levels locally by dissociating a β_1AR-PDE4 complex, thereby reducing the local cAMP-hydrolytic activity (***Richter et al., 2013***), β_1AR and β_2AR thus could utilize different mechanisms for β-blocker-induced signaling. Another interesting observation is that the β-blocker-induced β_2AR-cAMP signal is sufficient to promote PKA phosphorylation of both β_2AR and the receptor-associated $Ca_V1.2$ of LTCC,

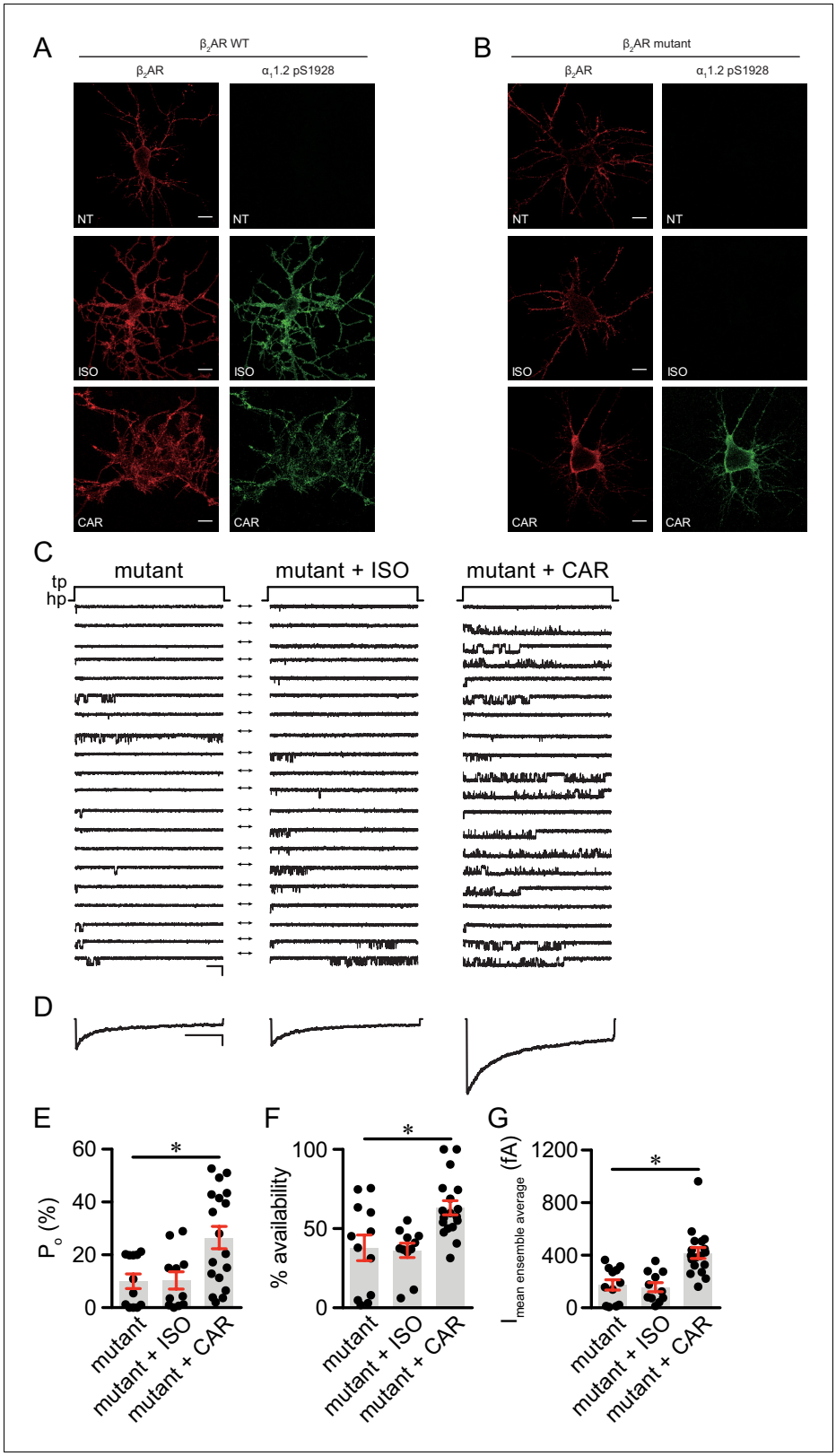

Figure 7. The β_2AR mutant selectively supports carvedilol-induced augmentation of LTCC activity in neurons. (**A–B**) β_1AR/β_2AR double knockout (DKO) mouse hippocampal neurons on 7–10 days in vitro (DIV) were cotransfected with FLAG-tagged β_2AR WT (**A**) or mutant (**B**) and HA-tagged LTCC $\alpha_1$1.2 subunit, 24 hr later cells were either mock treated (NT), or treated for 5 min with 10 nM isoproterenol (ISO) or carvedilol (CAR), fixed and labeled with

Figure 7 continued on next page

Figure 7 continued

anti-FLAG and a phospho-specific antibody for S1928 phosphorylated $\alpha_1$1.2. Confocal images show mutant β_2AR losts the ability of promoting LTCC phosphorylation upon ISO stimulation but remained the ability upon CAR stimulation in neurons. Scale bar, 10 μm. Representative of 6 images for each condition, three experiments. (**C**) Representative single channel recordings of LTCC Ca_V1.2 currents using 110 mM Ba^{2+} as charge carrier in DKO neurons on 7–10.days DIV expressing mutant β_2AR after depolarization from −80 to 0 mV in in control patches (mutant) and patches containing 1 μM isoproterenol (ISO) or 1 μM carvedilol (CAR) in the patch pipette. Shown are 20 consecutive sweeps from representative experiments. Arrows throughout the figure indicate the 0-current level (closed channel). Scale bar denotes 2 pA and 200 ms. (**D**) Ensemble average currents as determined from all sweeps recorded for all the experimental conditions. Scale bar denotes 50 fA and 400 ms. (**E–G**) Mean ± s.e.m. for (**E**) P_o (%), (**F**) availability (i.e. likelihood that a sweep had at least one event) (%) and (**G**) the mean ensemble average current (fA) for each experimental condition. *p<0.05 with Kruskal Wallis – Dunn's multiple comparison test. Sweep and n numbers as well as summary statistics are in ***Supplementary file 2***.

The online version of this article includes the following source data and figure supplement(s) for figure 7:

Source data 1. Excel spreadsheet containing the individual numeric values of Po, availability and current analyzed in ***Figure 7E-G***.

Figure supplement 1. The mutant β_2AR is selectively activated by carvedilol and promotes LTCC phosphorylation in neurons.

but not another substrate, the AMPAR GluA1 subunit. Both LTCC and AMPAR are shown to associate with the β_2AR in hippocampal neurons (***Davare et al., 2001***; ***Joiner et al., 2010***; ***Wang et al., 2010***; ***Qian et al., 2012***). Therefore, the preference of one local membrane target over another local target indicates a highly restricted nature of the cAMP-PKA activities, potentially dependent on the recently identified distinct subpopulations of β_2AR and associated signaling molecules in the neurons (***Shen et al., 2018***). Nevertheless, the PKA phosphorylation leads to augmentation of LTCC activity, potentially contributing to the neuronal toxicities. Therefore, activation of GPCR at low ligand concentrations should be taken into consideration when designing and screening new therapeutic drugs.

Materials and methods

Key resources table

Reagent type (species) or resource	Designation	Source or reference	Identifiers	Additional information
Strain (*Mus musculus*)	β_1AR/β_2AR double knockout	Jackson Laboratories	Stock # 003810	
Strain (*Rattus norvegicus*)	Sprague Dawley	Charles River Laboratories		
Cell line (*Homo sapiens*)	HEK293/β_2AR-WT	***De Arcangelis et al., 2009***		HEK293 cells stably expressing FLAG-β_2AR
Cell line (*Homo sapiens*)	HEK293/β_2AR-S204/207A	This paper		HEK293 cells stably expressing FLAG-β_2AR-S204/207A
Antibody	Phospho-β_2AR (Ser261/262) (mouse monoclonal)	Dr. Richard Clark (UT Huston)	Clone 2G3	IF (1 μg/ml), WB (1:1000)
Antibody	Phospho-β_2AR (Ser355/356) (mouse monoclonal)	Dr. Richard Clark (UT Huston)	Clone 10A5	WB (1:1000)
Antibody	β_2AR (rabbit polyclonal)	Santa Cruz Biotechnology	sc-570 RRID:AB_2225412	PLA (1:100), WB (1:1000)
Antibody	Phospho-β_2AR (Ser355/356) (rabbit polyclonal)	Santa Cruz Biotechnology	sc-16719R RRID:AB_781609	WB (1:1000)

Continued on next page

Continued

Reagent type (species) or resource	Designation	Source or reference	Identifiers	Additional information
Antibody	$\alpha_1$1.2 (rabbit polyclonal)	***Patriarchi et al., 2016***	FP1	WB (1:1000)
Antibody	Phospho-$\alpha_1$1.2 (Ser1928) (rabbit polyclonal)	***Patriarchi et al., 2016***	CH3P	IF (1 µg/ml), WB (1:1000)
Antibody	Phospho-$\alpha_1$1.2 (Ser1700) (rabbit polyclonal)	***Patriarchi et al., 2016***, Originally from Dr. William Catterall (U of Washington)		WB (1:1000)
Antibody	GluA1 (rabbit polyclonal)	***Patriarchi et al., 2016***		WB (1:1000)
Antibody	Phospho-GluA1 (Ser831) (rabbit polyclonal)	***Patriarchi et al., 2016***		WB (1:1000)
Antibody	Phospho-GluA1 (Ser845) (rabbit polyclonal)	***Patriarchi et al., 2016***		WB (1:1000)
Antibody	FLAG-M1	Sigma-Aldrich	F3040 RRID:AB_439712	IF (1 µg/ml), WB (1:1000)
Antibody	HA	Covance	MMS-101R RRID:AB_291262	PLA (1:1000)
Recombinant DNA reagent	β_2AR-mutant	This paper		FLAG-tagged human β_2AR with S204/207A double mutations
Recombinant DNA reagent	β_2AR-ICUE3	This paper		ICUE3 fused to the C-terminal of human β_2AR
Commercial assay or kit	Duolink in situ detection reagents	Sigma-Aldrich	DUO92007	PLA
Software, algorithm	pCLAMP10	Molecular Devices		electrophysiology
Software, algorithm	MetaFluor	Molecular Devices		FRET

Animals

β_1AR/β_2AR double knockout (DKO) mouse were obtained from Jackson Laboratories to produce P0-P1 postnatal DKO pups, SD pregnant rats were obtained from Charles River Laboratories to provide E17-E19 embryonic rats. All of the animals were handled according to approved institutional animal care and use committee (IACUC) protocols (#20234 and #20673) of the University of California at Davis and in accordance with the NIH guidelines.

Plasmids

DNA constructs expressing FLAG-tagged human β_2AR (FLAG-β_2AR) and HA-tagged rat L-type calcium channel (LTCC) $\alpha_1$1.2 were described before (***Shen et al., 2018***). FLAG-tagged human β_2AR with S204/207A double mutations (FLAG-mutant) was generated by Gibson assembly method (Thermo Fisher) using FLAG-β_2AR and synthetic gBlocks with the double mutations as templates (Integrated DNA Technologies). FRET biosensor ICUE3, CAAX-ICUE3 and LYN-ICUE3 were described before (***DiPilato and Zhang, 2009***). To make the β_2AR-ICUE3 fusion biosensor, ICUE3 was fused to the C-terminal of FLAG-β_2AR with Gly-Ser linker. HA-Gsα was made by replacing CFP with HA tag, using Gsα-CFP as template (a gift from Dr. Catherine Berlot, Addgene plasmid # 55793).

Antibodies and chemicals

Mouse monoclonal antibodies against β_2AR at serine 261/262 (clone 2G3) and at serine 355/356 (clone 10A5) were kindly provided by Dr. Richard Clark (UT Huston). Polyclonal antibodies against β_2AR (sc-570) and phosphorylated β_2AR at serine 355/356 (sc-16719R) were purchased from Santa Cruz Biotechnology. Polyclonal antibodies against $\alpha_1$1.2 residues 754–901 for total $\alpha_1$1.2 (FP1), residues 1923–1935 for phosphorylated serine 1928 site (LGRRApSFHLECLK, pS1928) and residues 1694–1709 for phosphorylated serine 1700 site (EIRRAIpSGDLTAEEEL, pS1700) were described before (***Patriarchi et al., 2016***). Polyclonal antibodies against GluA1 residues 894–907 for total GluA1, residues 826–837 for phosphorylated serine 831 site (LIPQQpSINEAIK, pS831) and residues 840–851 for phosphorylated serine 845 site (TLPRNpSGAGASK, pS845) were described before (***Patriarchi et al., 2016***). Other antibodies used in the experiments include: anti-FLAG (F3040, Sigma), anti-HA (MMS-101R, Covance), Alexa fluor 488 conjugated goat anti-rabbit IgG and Alexa fluor 594 conjugated goat anti-mouse IgG (A-11034 and A-11032, Thermo Fisher), DyLight 680 conjugated goat anti-mouse IgG and anti-rabbit IgG (35518 and 35568, Thermo Fisher), IRDye 800CW conjugated goat anti-mouse IgG and anti-rabbit IgG (926–32210 and 926–32211, Li-cor).

Isoproterenol (I2760), timolol (T6394), alprenolol (A8676), propranolol (P0884), metoprolol (M5391), CGP12177A (C125), CGP20712A (C231), ICI118551 (I127), 3-isobutyl-1-methylxanthine (I5879) and 2',5'-dideoxyadenosine (D7408) were purchased from Sigma. Carvedilol (15418) was from Cayman Chemical, H89 (H-5239) was from LC Labs, pertussis toxin (179B) was from List Labs.

Cell culture and transfection

Human embryonic kidney HEK293 cells were from American Type Culture Collection (ATCC) and were maintained in Dulbecco's modified Eagle medium (DMEM, Corning) supplemented with 10% fetal bovine serum (FBS, Sigma). HEK293 cells stably expressing FLAG-β_2AR was from previous study (***De Arcangelis et al., 2009***). HEK293 cells stably expressing FLAG-mutant β_2AR was generated in this study. Briefly, cells transfected with β_2AR-mutant were selected by G418 resistance (Corning) and cell clones were obtained by limiting serial dilution, monoclonal cells were analyzed by western blots and the one with comparable β_2AR expression to FLAG-β_2AR stable cells was chosen.

Mouse embryonic fibroblasts (MEFs) from β_1AR/β_2AR double knockout (DKO) mouse were described in previous study (***Cervantes et al., 2010***) and were maintained in DMEM supplemented with 10% FBS. Primary mouse hippocampal neurons were isolated and cultured from P0-P1 early postnatal DKO mouse pups, and primary rat hippocampal neurons were prepared from E17-E19 embryonic rats using methods described previously (***Chen et al., 2008***; ***Beaudoin et al., 2012***). Briefly, dissected hippocampi were dissociated by 0.25% trypsin (Corning) and trituration. Neurons were plated on poly-D-lysine-coated (Sigma) glass coverslips in 24-well plate for imaging and in 6-well plate for biochemistry at a cell density of 50,000/well and 1 million/well, respectively. Neurons were cultured in Neurobasal medium supplemented with GlutaMax and B-27 (Thermo Fisher).

HEK293 cells were transfected with plasmids using polyethylenimine according to manufacturer's instructions (Sigma). Neurons were transfected by the Ca^{2+}-phosphate method (***Jiang and Chen, 2006***). Briefly, cultured neurons on 6–10 DIV were switched to pre-warmed Eagle's minimum essential medium (EMEM, Thermo Fisher) supplemented with GlutaMax 1 hr before transfection, conditioned media were saved. DNA precipitates were prepared by 2x HBS (pH 6.96) and 2 M $CaCl_2$. After incubation with DNA precipitates for 1 hr, neurons were incubated in 10% CO_2 pre-equilibrium EMEM for 20 min, then replaced with conditioned medium and cultured in 5% CO_2 incubator until use.

Confocal microscopy imaging

Rat hippocampal neurons were transfected with FLAG-β_2AR on 10 DIV, treated for 5 min with 10 nM or 1 µM indicated drugs on 12 DIV. Mouse DKO hippocampal neurons were transfected with FLAG-β_2AR or FLAG-mutant and HA-$\alpha_1$1.2 at 1:1 ratio on 6–8 DIV, and stimulated with indicated drugs and times 24 hr after transfection. Treated cells were fixed, permeabilized, and co-stained with indicated antibodies with a final concentration of 1 µg/ml for each antibody, which were revealed by a 1:1000 dilution of Alexa fluor 488 conjugated goat anti-rabbit IgG or Alexa fluor 594 conjugated goat anti-mouse IgG, respectively. Fluorescence images were taken by Zeiss LSM 700 confocal microscope with a 63×/1.4 numerical aperture oil-immersion lens.

Proximity ligation assay

HEK293 cells growing on poly-D-lysine coated coverslips were transfected with FLAG-β_2AR or FLAG-mutant, HA-Gsα and pEYFP-N1 at 8:1:1 ratio. 24 hr after transfection, cells were serum-starved 2 hr, treated 100 nM indicated drugs for 5 min. Following stimulation, cells were fixed, permeabilized, and co-stained with anti-β_2AR antibody (1:100 dilution) from rabbit in conjunction with anti-HA antibody (1:1000 dilution) from mouse. The proximity ligation reaction was performed according to the manufacturer's protocol using the Duolink in situ detection orange reagents (Sigma). Images were recorded with Zeiss LSM 700 confocal microscope with a 63×/1.4 numerical aperture oil-immersion lens. To quantify the PLA signals, the number of red fluorescent objects in each image was quantified using the Squassh plug-in for ImageJ software (***Rizk et al., 2014***), and divided by the number of transfected cells.

Fluorescence resonance energy transfer (FRET) measurement

FRET measurement was performed as previously described (***De Arcangelis et al., 2009***). Briefly, HEK 293 cells were transfected with ICUE3 or β_2AR-ICUE3, DKO MEFs were co-transfected with ICUE3 and FLAG-β_2AR or FLAG-mutant. Cells were imaged on a Zeiss Axiovert 200M microscope with a 40×/1.3 numerical aperture oil-immersion lens and a cooled CCD camera. Dual emission ratio imaging was acquired with a 420DF20 excitation filter, a 450DRLP diachronic mirror, and two emission filters (475DF40 for cyan and 535DF25 for yellow). The acquisition was set with 0.2 s exposure in both channels and 20 s elapses. Images in both channels were subjected to background subtraction, and ratios of yellow-to-cyan were calculated at different time points.

Western blot

HEK293 cells stably expressing FLAG-β_2AR or FLAG-mutant were serum-starved for 2 hr and treated with indicated drugs and times, then harvested by lysis buffer (10 mM Tris pH 7.4, 1% NP40, 150 mM NaCl, 2 mM EDTA) with protease and phosphatase inhibitor cocktail. Rat hippocampal neurons on 10–14 DIV were treated with indicated drugs and times, then harvested by lysis buffer (10 mM Tris pH 7.4, 1% TX-100, 150 mM NaCl, 5 mM EGTA, 10 mM EDTA, 10% glycerol) with protease and phosphatase inhibitor cocktail. Protein samples were analyzed by western blot using antibodies as indicated at a 1:1000 dilution and signals were detected by Odyssey scanner (Li-cor).

Cell-attached patch clamp electrophysiology

Primary rat and mouse hippocampal neurons were used on 7–10 DIV. Cell-attached patch clamp recordings were performed on an Olympus IX70 inverted microscope in a 15 mm culture coverslip at room temperature (22–25˚C). Signals were recorded at 10 kHz and low-pass filtered at 2 kHz with an Axopatch 200B amplifier and digitized with a Digidata 1440 (Molecular Devices). Recording pipettes were pulled from borosilicate capillary glass (0.86 OD) with a Flaming micropipette puller (Model P-97, Sutter Instruments) and polished (polisher from World Precision Instruments). Pipette resistances were strictly maintained between 6–7 MΩ to ameliorate variations in number of channels in the patch pipette. The patch transmembrane potential was zeroed by perfusing cells with a high K^+ extracellular solution containing (in mM) 145 KCl, 10 NaCl, and 10 HEPES, pH 7.4 (NaOH). The pipette solution contained (in mM) 20 tetraethylammonium chloride (TEA-Cl), 110 $BaCl_2$ (as charge carrier), and 10 HEPES, pH 7.3 (TEA-OH). This pipette solution was supplemented with 1 µM ω-conotoxin GVIA and 1 µM ω-conotoxin MCVIIC to block N and P/Q-type Ca^{2+} channels, respectively, and (S)-(-)-BayK-8644 (500 nM) was included in the pipette solution to promote longer open times and resolve channel openings as previously performed by our group and others (***Shen et al., 2018***; ***Davare et al., 2001***; ***Wang et al., 2001***; ***Qian et al., 2017***; ***Hess et al., 1986***; ***Schuhmann et al., 1997***; ***Costantin et al., 1998***; ***Yue and Marban, 1990***; ***Dzhura and Neely, 2003***; ***Navedo et al., 2005***). In a subset of experiments, BayK was left out of the pipette solution. Note that ISO and CAR had similar effects on channel activity whether BayK was included or not in the pipette solution. To examine the effects of β-adrenergic stimulation on the L-type $Ca_V1.2$ single-channel activity, 1 µM isoproterenol was added to the pipette solution in independent experiments. Note that we have previously used the L-type $Ca_V1.2$ channel blocker nifedipine (1 µM) to confirm the recording of L-type $Ca_V1.2$ currents under control conditions and in the presence of isoproterenol (***Patriarchi et al., 2016***). Single-channel activity was recorded during a single pulse protocol (2 s)

from a holding potential of −80 mV to 0 mV every 5 s. An average of >50 sweeps were collected with each recording file under all experimental conditions. The half-amplitude event-detection algorithm of pClamp10 was used to measure overall single-channel L-type $Ca_V1.2$ activity as nPo, where n is the number of channels in the patch and Po is the open probability. Because the variability of nPo can be a critical element to interpret single channel data due to overstating open probability based on a high n number, we corrected this parameter by the number of channels (n) describing channel open probability and availability as well as calculating the mean ensemble average current. Data were pooled for each condition and analyzed with GraphPad Prism software.

Statistical analysis

Data were analyzed using GraphPad Prism software and expressed as mean ± s.e.m. Differences between two groups were assessed by appropriate two-tailed unpaired Student's t-test or nonparametric Mann-Whitney test. Differences among three or more groups were assessed by One-way ANOVA with Tukey's post hoc test or the Kruskal-Wallis test with Dunn's post hoc test. $p<0.05$ was considered statistically significant (denoted by * or # in figures).

Data availability

All data generated or analyzed during this study are included in the manuscript and supporting files. Source data files have been provided for all main figures.

Acknowledgements

This work was supported by NIH grant GM129376 and VA Merit grant BX002900 to YKX, and NIH grants HL098200, HL121059 and HL149127 to MFN. AS and QS were recipients of AHA postdoctoral fellowship. YKX is an established AHA investigator.

Additional information

Funding

Funder	Grant reference number	Author
National Institutes of Health	GM129376	Yang K Xiang
U.S. Department of Veterans Affairs	BX002900	Yang K Xiang
National Institutes of Health	HL098200	Manuel F Navedo
National Institutes of Health	HL121059	Manuel F Navedo
National Institutes of Health	HL149127	Manuel F Navedo
American Heart Association	Postdoctoral fellowship	Ao Shen Qian Shi
American Heart Association		Yang K Xiang

The funders had no role in study design, data collection and interpretation, or the decision to submit the work for publication.

Author contributions

Ao Shen, Conceptualization, Data curation, Formal analysis, Writing—original draft, Writing—review and editing; Dana Chen, Manpreet Kaur, Peter Bartels, Bing Xu, Qian Shi, Joseph M Martinez, Madeline Nieves-Cintron, Data curation; Kwun-nok Mimi Man, Resources; Johannes W Hell, Supervision, Writing—review and editing; Manuel F Navedo, Data curation, Formal analysis, Writing—review and editing; Xi-Yong Yu, Supervision; Yang K Xiang, Conceptualization, Formal analysis, Supervision, Funding acquisition, Writing—original draft, Writing—review and editing

Author ORCIDs

Ao Shen https://orcid.org/0000-0002-1559-3895
Johannes W Hell http://orcid.org/0000-0001-7960-7531
Manuel F Navedo http://orcid.org/0000-0001-6864-6594
Yang K Xiang https://orcid.org/0000-0003-1786-9143

Ethics

Animal experimentation: This study was performed in strict accordance with the recommendations in the Guide for the Care and Use of Laboratory Animals of the National Institutes of Health. All of the animals were handled according to approved institutional animal care and use committee (IACUC) protocols (#20234) of the University of California at Davis. Every effort was made to minimize suffering.

Decision letter and Author response

Decision letter https://doi.org/10.7554/eLife.49464.sa1
Author response https://doi.org/10.7554/eLife.49464.sa2

Additional files

Supplementary files

- Supplementary file 1. Biophysical properties of L-type Ca^{2+} currents in the neurons recorded in ***Figure 5A–5E***.Values are mean ± SEM. *p<0.05 with Kruskal Wallis – Dunn's multiple comparison test.
- Supplementary file 2. Biophysical properties of L-type Ca^{2+} currents in the neurons recorded in ***Figure 7C–7G***.Values are mean ± SEM. *p<0.05 with Kruskal Wallis – Dunn's multiple comparison test.
- Transparent reporting form

Data availability

All data generated or analyzed during this study are included in the manuscript and supporting files. Source data files have been provided for all main figures.

References

Bakris G. 2009. An in-depth analysis of vasodilation in the management of hypertension: focus on adrenergic blockade. *Journal of Cardiovascular Pharmacology* **53**:379–387. DOI: https://doi.org/10.1097/FJC.0b013e31819fd501, PMID: 19454898

Beaudoin GM, Lee SH, Singh D, Yuan Y, Ng YG, Reichardt LF, Arikkath J. 2012. Culturing pyramidal neurons from the early postnatal mouse Hippocampus and cortex. *Nature Protocols* **7**:1741–1754. DOI: https://doi.org/10.1038/nprot.2012.099, PMID: 22936216

Brixius K, Bundkirchen A, Bölck B, Mehlhorn U, Schwinger RH. 2001. Nebivolol, bucindolol, metoprolol and carvedilol are devoid of intrinsic sympathomimetic activity in human myocardium. *British Journal of Pharmacology* **133**:1330–1338. DOI: https://doi.org/10.1038/sj.bjp.0704188, PMID: 11498519

Cervantes D, Crosby C, Xiang Y. 2010. Arrestin orchestrates crosstalk between G protein-coupled receptors to modulate the spatiotemporal activation of ERK MAPK. *Circulation Research* **106**:79–88. DOI: https://doi.org/10.1161/CIRCRESAHA.109.198580, PMID: 19926878

Chen Y, Stevens B, Chang J, Milbrandt J, Barres BA, Hell JW. 2008. NS21: re-defined and modified supplement B27 for neuronal cultures. *Journal of Neuroscience Methods* **171**:239–247. DOI: https://doi.org/10.1016/j.jneumeth.2008.03.013, PMID: 18471889

Choi M, Staus DP, Wingler LM, Ahn S, Pani B, Capel WD, Lefkowitz RJ. 2018. G protein-coupled receptor kinases (GRKs) orchestrate biased agonism at the β_2-adrenergic receptor. *Science Signaling* **11**:eaar7084. DOI: https://doi.org/10.1126/scisignal.aar7084, PMID: 30131371

Civciristov S, Ellisdon AM, Suderman R, Pon CK, Evans BA, Kleifeld O, Charlton SJ, Hlavacek WS, Canals M, Halls ML. 2018. Preassembled GPCR signaling complexes mediate distinct cellular responses to ultralow ligand concentrations. *Science Signaling* **11**:eaan1188. DOI: https://doi.org/10.1126/scisignal.aan1188, PMID: 30301787

Costantin J, Noceti F, Qin N, Wei X, Birnbaumer L, Stefani E. 1998. Facilitation by the beta2a subunit of pore openings in cardiac $^{Ca2+}$ channels. *The Journal of Physiology* **507 (Pt 1**:93–103. DOI: https://doi.org/10.1111/j.1469-7793.1998.093bu.x, PMID: 9490822

Daaka Y, Luttrell LM, Lefkowitz RJ. 1997. Switching of the coupling of the beta2-adrenergic receptor to different G proteins by protein kinase A. *Nature* **390**:88–91. DOI: https://doi.org/10.1038/36362, PMID: 9363896

Davare MA, Avdonin V, Hall DD, Peden EM, Burette A, Weinberg RJ, Horne MC, Hoshi T, Hell JW. 2001. A beta2 adrenergic receptor signaling complex assembled with the Ca2+ channel Cav1.2. *Science* **293**:98–101. DOI: https://doi.org/10.1126/science.293.5527.98, PMID: 11441182

De Arcangelis V, Liu R, Soto D, Xiang Y. 2009. Differential association of phosphodiesterase 4D isoforms with beta2-adrenoceptor in cardiac myocytes. *The Journal of Biological Chemistry* **284**:33824–33832. DOI: https://doi.org/10.1074/jbc.M109.020388, PMID: 19801680

DeVree BT, Mahoney JP, Vélez-Ruiz GA, Rasmussen SG, Kuszak AJ, Edwald E, Fung JJ, Manglik A, Masureel M, Du Y, Matt RA, Pardon E, Steyaert J, Kobilka BK, Sunahara RK. 2016. Allosteric coupling from G protein to the agonist-binding pocket in GPCRs. *Nature* **535**:182–186. DOI: https://doi.org/10.1038/nature18324, PMID: 27362234

DiPilato LM, Zhang J. 2009. The role of membrane microdomains in shaping beta2-adrenergic receptor-mediated cAMP dynamics. *Molecular BioSystems* **5**:832–837. DOI: https://doi.org/10.1039/b823243a, PMID: 19603118

Dzhura I, Neely A. 2003. Differential modulation of cardiac $^{Ca2+}$channel gating by beta-subunits. *Biophysical Journal* **85**:274–289. DOI: https://doi.org/10.1016/S0006-3495(03)74473-7, PMID: 12829483

Eichel K, Jullié D, Barsi-Rhyne B, Latorraca NR, Masureel M, Sibarita JB, Dror RO, von Zastrow M. 2018. Catalytic activation of β-arrestin by GPCRs. *Nature* **557**:381–386. DOI: https://doi.org/10.1038/s41586-018-0079-1, PMID: 29720660

Fu Q, Shi Q, West TM, Xiang YK. 2017. Cross-Talk between insulin signaling and G Protein-Coupled receptors. *Journal of Cardiovascular Pharmacology* **70**:74–86. DOI: https://doi.org/10.1097/FJC.0000000000000481, PMID: 28328746

Gorre F, Vandekerckhove H. 2010. Beta-blockers: focus on mechanism of action. Which beta-blocker, when and why? *Acta Cardiologica* **65**:565–570. DOI: https://doi.org/10.1080/AC.65.5.2056244, PMID: 21125979

Gregorio GG, Masureel M, Hilger D, Terry DS, Juette M, Zhao H, Zhou Z, Perez-Aguilar JM, Hauge M, Mathiasen S, Javitch JA, Weinstein H, Kobilka BK, Blanchard SC. 2017. Single-molecule analysis of ligand efficacy in β_2AR-G-protein activation. *Nature* **547**:68–73. DOI: https://doi.org/10.1038/nature22354, PMID: 28607487

Grundmann M, Merten N, Malfacini D, Inoue A, Preis P, Simon K, Rüttiger N, Ziegler N, Benkel T, Schmitt NK, Ishida S, Müller I, Reher R, Kawakami K, Inoue A, Rick U, Kühl T, Imhof D, Aoki J, König GM, et al. 2018. Lack of beta-arrestin signaling in the absence of active G proteins. *Nature Communications* **9**:341. DOI: https://doi.org/10.1038/s41467-017-02661-3, PMID: 29362459

Hess P, Lansman JB, Tsien RW. 1986. Calcium channel selectivity for divalent and monovalent cations. Voltage and concentration dependence of single channel current in ventricular heart cells. *The Journal of General Physiology* **88**:293–319. DOI: https://doi.org/10.1085/jgp.88.3.293, PMID: 2428919

Jiang M, Chen G. 2006. High Ca2+-phosphate transfection efficiency in low-density neuronal cultures. *Nature Protocols* **1**:695–700. DOI: https://doi.org/10.1038/nprot.2006.86, PMID: 17406298

Joiner ML, Lisé MF, Yuen EY, Kam AY, Zhang M, Hall DD, Malik ZA, Qian H, Chen Y, Ulrich JD, Burette AC, Weinberg RJ, Law PY, El-Husseini A, Yan Z, Hell JW. 2010. Assembly of a β2-adrenergic receptor—GluR1 signalling complex for localized cAMP signalling. *The EMBO Journal* **29**:482–495. DOI: https://doi.org/10.1038/emboj.2009.344, PMID: 19942860

Kim J, Ahn S, Ren XR, Whalen EJ, Reiter E, Wei H, Lefkowitz RJ. 2005. Functional antagonism of different G protein-coupled receptor kinases for beta-arrestin-mediated angiotensin II receptor signaling. *PNAS* **102**:1442–1447. DOI: https://doi.org/10.1073/pnas.0409532102, PMID: 15671181

Kim IM, Tilley DG, Chen J, Salazar NC, Whalen EJ, Violin JD, Rockman HA. 2008. Beta-blockers alprenolol and carvedilol stimulate beta-arrestin-mediated EGFR transactivation. *PNAS* **105**:14555–14560. DOI: https://doi.org/10.1073/pnas.0804745105, PMID: 18787115

Larochelle P, Tobe SW, Lacourcière Y. 2014. β-Blockers in hypertension: studies and meta-analyses over the years. *Canadian Journal of Cardiology* **30**:S16–S22. DOI: https://doi.org/10.1016/j.cjca.2014.02.012, PMID: 24750978

Lee HM, Giguere PM, Roth BL. 2014. DREADDs: novel tools for drug discovery and development. *Drug Discovery Today* **19**:469–473. DOI: https://doi.org/10.1016/j.drudis.2013.10.018, PMID: 24184433

Lefkowitz RJ. 2000. The superfamily of heptahelical receptors. *Nature Cell Biology* **2**:E133–E136. DOI: https://doi.org/10.1038/35017152, PMID: 10878827

Lefkowitz RJ. 2007. Seven transmembrane receptors: something old, something new. *Acta Physiologica* **190**:9–19. DOI: https://doi.org/10.1111/j.1365-201X.2007.01693.x, PMID: 17428228

Liapakis G, Ballesteros JA, Papachristou S, Chan WC, Chen X, Javitch JA. 2000. The forgotten serine. A critical role for Ser-2035.42 in ligand binding to and activation of the beta 2-adrenergic receptor. *The Journal of Biological Chemistry* **275**:37779–37788. DOI: https://doi.org/10.1074/jbc.M002092200, PMID: 10964911

Liu R, Ramani B, Soto D, De Arcangelis V, Xiang Y. 2009. Agonist dose-dependent phosphorylation by protein kinase A and G protein-coupled receptor kinase regulates beta2 adrenoceptor coupling to G(i) proteins in cardiomyocytes. *The Journal of Biological Chemistry* **284**:32279–32287. DOI: https://doi.org/10.1074/jbc.M109.021428, PMID: 19706594

Luttrell LM, Ferguson SS, Daaka Y, Miller WE, Maudsley S, Della Rocca GJ, Lin F, Kawakatsu H, Owada K, Luttrell DK, Caron MG, Lefkowitz RJ. 1999. Beta-arrestin-dependent formation of beta2 adrenergic receptor-Src protein kinase complexes. *Science* **283**:655–661. DOI: https://doi.org/10.1126/science.283.5402.655, PMID: 9924018

Maack C, Cremers B, Flesch M, Höper A, Südkamp M, Böhm M. 2000. Different intrinsic activities of bucindolol, carvedilol and metoprolol in human failing myocardium. *British Journal of Pharmacology* **130**:1131–1139. DOI: https://doi.org/10.1038/sj.bjp.0703400, PMID: 10882399

Mammarella N, Di Domenico A, Palumbo R, Fairfield B. 2016. Noradrenergic modulation of emotional memory in aging. *Ageing Research Reviews* **27**:61–66. DOI: https://doi.org/10.1016/j.arr.2016.03.004, PMID: 27003374

Matera MG, Page C, Rinaldi B. 2018. β2-Adrenoceptor signalling Bias in asthma and COPD and the potential impact on the comorbidities associated with these diseases. *Current Opinion in Pharmacology* **40**:142–146. DOI: https://doi.org/10.1016/j.coph.2018.04.012, PMID: 29763833

Najafi A, Sequeira V, Kuster DW, van der Velden J. 2016. β-adrenergic receptor signalling and its functional consequences in the diseased heart. *European Journal of Clinical Investigation* **46**:362–374. DOI: https://doi.org/10.1111/eci.12598, PMID: 26842371

Navedo MF, Amberg GC, Votaw VS, Santana LF. 2005. Constitutively active L-type $^{Ca2+}$ channels. *PNAS* **102**: 11112–11117. DOI: https://doi.org/10.1073/pnas.0500360102, PMID: 16040810

Nobles KN, Xiao K, Ahn S, Shukla AK, Lam CM, Rajagopal S, Strachan RT, Huang TY, Bressler EA, Hara MR, Shenoy SK, Gygi SP, Lefkowitz RJ. 2011. Distinct phosphorylation sites on the β(2)-adrenergic receptor establish a barcode that encodes differential functions of β-arrestin. *Science Signaling* **4**:ra51. DOI: https://doi.org/10.1126/scisignal.2001707, PMID: 21868357

Patriarchi T, Qian H, Di Biase V, Malik ZA, Chowdhury D, Price JL, Hammes EA, Buonarati OR, Westenbroek RE, Catterall WA, Hofmann F, Xiang YK, Murphy GG, Chen CY, Navedo MF, Hell JW. 2016. Phosphorylation of Cav1.2 on S1928 uncouples the L-type Ca2+ channel from the β2 adrenergic receptor. *The EMBO Journal* **35**: 1330–1345. DOI: https://doi.org/10.15252/embj.201593409, PMID: 27103070

Pierce KL, Maudsley S, Daaka Y, Luttrell LM, Lefkowitz RJ. 2000. Role of endocytosis in the activation of the extracellular signal-regulated kinase cascade by sequestering and nonsequestering G protein-coupled receptors. *PNAS* **97**:1489–1494. DOI: https://doi.org/10.1073/pnas.97.4.1489, PMID: 10677489

Qian H, Matt L, Zhang M, Nguyen M, Patriarchi T, Koval OM, Anderson ME, He K, Lee HK, Hell JW. 2012. β2-Adrenergic receptor supports prolonged theta tetanus-induced LTP. *Journal of Neurophysiology* **107**:2703–2712. DOI: https://doi.org/10.1152/jn.00374.2011, PMID: 22338020

Qian H, Patriarchi T, Price JL, Matt L, Lee B, Nieves-Cintrón M, Buonarati OR, Chowdhury D, Nanou E, Nystoriak MA, Catterall WA, Poomvanicha M, Hofmann F, Navedo MF, Hell JW. 2017. Phosphorylation of Ser1928 mediates the enhanced activity of the L-type Ca2+ channel Cav1.2 by the β2-adrenergic receptor in neurons. *Science Signaling* **10**:eaaf9659. DOI: https://doi.org/10.1126/scisignal.aaf9659, PMID: 28119465

Reiter E, Lefkowitz RJ. 2006. GRKs and beta-arrestins: roles in receptor silencing, trafficking and signaling. *Trends in Endocrinology & Metabolism* **17**:159–165. DOI: https://doi.org/10.1016/j.tem.2006.03.008, PMID: 16595179

Ren XR, Reiter E, Ahn S, Kim J, Chen W, Lefkowitz RJ. 2005. Different G protein-coupled receptor kinases govern G protein and beta-arrestin-mediated signaling of V2 vasopressin receptor. *PNAS* **102**:1448–1453. DOI: https://doi.org/10.1073/pnas.0409534102, PMID: 15671180

Richter W, Mika D, Blanchard E, Day P, Conti M. 2013. β1-adrenergic receptor antagonists signal via PDE4 translocation. *EMBO Reports* **14**:276–283. DOI: https://doi.org/10.1038/embor.2013.4, PMID: 23381222

Ring AM, Manglik A, Kruse AC, Enos MD, Weis WI, Garcia KC, Kobilka BK. 2013. Adrenaline-activated structure of β2-adrenoceptor stabilized by an engineered nanobody. *Nature* **502**:575–579. DOI: https://doi.org/10.1038/nature12572, PMID: 24056936

Rizk A, Paul G, Incardona P, Bugarski M, Mansouri M, Niemann A, Ziegler U, Berger P, Sbalzarini IF. 2014. Segmentation and quantification of subcellular structures in fluorescence microscopy images using squassh. *Nature Protocols* **9**:586–596. DOI: https://doi.org/10.1038/nprot.2014.037, PMID: 24525752

Schuhmann K, Romanin C, Baumgartner W, Groschner K. 1997. Intracellular Ca2+ inhibits smooth muscle L-type Ca2+ channels by activation of protein phosphatase type 2B and by direct interaction with the channel. *The Journal of General Physiology* **110**:503–513. DOI: https://doi.org/10.1085/jgp.110.5.503, PMID: 9348323

Shen A, Nieves-Cintron M, Deng Y, Shi Q, Chowdhury D, Qi J, Hell JW, Navedo MF, Xiang YK. 2018. Functionally distinct and selectively phosphorylated GPCR subpopulations co-exist in a single cell. *Nature Communications* **9**:1050. DOI: https://doi.org/10.1038/s41467-018-03459-7, PMID: 29535304

Shenoy SK, Drake MT, Nelson CD, Houtz DA, Xiao K, Madabushi S, Reiter E, Premont RT, Lichtarge O, Lefkowitz RJ. 2006. beta-arrestin-dependent, G protein-independent ERK1/2 activation by the beta2 adrenergic receptor. *Journal of Biological Chemistry* **281**:1261–1273. DOI: https://doi.org/10.1074/jbc.M506576200, PMID: 16280323

Strader CD, Candelore MR, Hill WS, Sigal IS, Dixon RA. 1989. Identification of two serine residues involved in agonist activation of the beta-adrenergic receptor. *The Journal of Biological Chemistry* **264**:13572–13578. PMID: 2547766

Tran TM, Friedman J, Qunaibi E, Baameur F, Moore RH, Clark RB. 2004. Characterization of agonist stimulation of cAMP-dependent protein kinase and G protein-coupled receptor kinase phosphorylation of the beta2-adrenergic receptor using phosphoserine-specific antibodies. *Molecular Pharmacology* **65**:196–206. DOI: https://doi.org/10.1124/mol.65.1.196, PMID: 14722251

Tran TM, Friedman J, Baameur F, Knoll BJ, Moore RH, Clark RB. 2007. Characterization of beta2-adrenergic receptor dephosphorylation: comparison with the rate of resensitization. *Molecular Pharmacology* **71**:47–60. DOI: https://doi.org/10.1124/mol.106.028456, PMID: 17012621

Wang SQ, Song LS, Lakatta EG, Cheng H. 2001. Ca2+ signalling between single L-type Ca2+ channels and ryanodine receptors in heart cells. *Nature* **410**:592–596. DOI: https://doi.org/10.1038/35069083, PMID: 11279498

Wang D, Govindaiah G, Liu R, De Arcangelis V, Cox CL, Xiang YK. 2010. Binding of amyloid beta peptide to beta2 adrenergic receptor induces PKA-dependent AMPA receptor hyperactivity. *FASEB Journal : Official Publication of the Federation of American Societies for Experimental Biology* **24**:3511–3521. DOI: https://doi.org/10.1096/fj.10-156661, PMID: 20395454

Wang J, Hanada K, Staus DP, Makara MA, Dahal GR, Chen Q, Ahles A, Engelhardt S, Rockman HA. 2017. $G\alpha_i$ is required for carvedilol-induced β_1 adrenergic receptor β-arrestin biased signaling. *Nature Communications* **8**:1706. DOI: https://doi.org/10.1038/s41467-017-01855-z, PMID: 29167435

Warne T, Edwards PC, Leslie AG, Tate CG. 2012. Crystal structures of a stabilized β1-adrenoceptor bound to the biased agonists bucindolol and carvedilol. *Structure* **20**:841–849. DOI: https://doi.org/10.1016/j.str.2012.03.014, PMID: 22579251

Wisler JW, DeWire SM, Whalen EJ, Violin JD, Drake MT, Ahn S, Shenoy SK, Lefkowitz RJ. 2007. A unique mechanism of beta-blocker action: carvedilol stimulates beta-arrestin signaling. *PNAS* **104**:16657–16662. DOI: https://doi.org/10.1073/pnas.0707936104, PMID: 17925438

Wisler JW, Xiao K, Thomsen AR, Lefkowitz RJ. 2014. Recent developments in biased agonism. *Current Opinion in Cell Biology* **27**:18–24. DOI: https://doi.org/10.1016/j.ceb.2013.10.008, PMID: 24680426

Xiang Y, Kobilka BK. 2003. Myocyte adrenoceptor signaling pathways. *Science* **300**:1530–1532. DOI: https://doi.org/10.1126/science.1079206, PMID: 12791980

Yao XJ, Vélez Ruiz G, Whorton MR, Rasmussen SG, DeVree BT, Deupi X, Sunahara RK, Kobilka B. 2009. The effect of ligand efficacy on the formation and stability of a GPCR-G protein complex. *PNAS* **106**:9501–9506. DOI: https://doi.org/10.1073/pnas.0811437106, PMID: 19470481

Yue DT, Marban E. 1990. Permeation in the dihydropyridine-sensitive calcium channel. Multi-ion occupancy but no anomalous mole-fraction effect between $^{Ba2+}$ and Ca2+. *The Journal of General Physiology* **95**:911–939. DOI: https://doi.org/10.1085/jgp.95.5.911, PMID: 2163433

Zamah AM, Delahunty M, Luttrell LM, Lefkowitz RJ. 2002. Protein kinase A-mediated phosphorylation of the beta 2-adrenergic receptor regulates its coupling to gs and gi. Demonstration in a reconstituted system. *The Journal of Biological Chemistry* **277**:31249–31256. DOI: https://doi.org/10.1074/jbc.M202753200, PMID: 12063255

Zidar DA, Violin JD, Whalen EJ, Lefkowitz RJ. 2009. Selective engagement of G protein coupled receptor kinases (GRKs) encodes distinct functions of biased ligands. *PNAS* **106**:9649–9654. DOI: https://doi.org/10.1073/pnas.0904361106, PMID: 19497875

Zweemer AJ, Toraskar J, Heitman LH, IJzerman AP. 2014. Bias in chemokine receptor signalling. *Trends in Immunology* **35**:243–252. DOI: https://doi.org/10.1016/j.it.2014.02.004, PMID: 24679437